On the theory of barrierless electronic relaxation in solution

Biman Bagchi

Citation: The Journal of Chemical Physics **87**, 5393 (1987); doi: 10.1063/1.453658
View online: http://dx.doi.org/10.1063/1.453658
View Table of Contents: http://scitation.aip.org/content/aip/journal/jcp/87/9?ver=pdfcov
Published by the AIP Publishing

On the theory of barrierless electronic relaxation in solution[a)]

Biman Bagchi
Solid State and Structural Chemistry Unit, Indian Institute of Science, Bangalore 560012, India

(Received 21 April 1987; accepted 29 July 1987)

We report a theoretical study of the barrierless electronic relaxation in solution. The existing theoretical models are divided into two classes: (A) Instantaneous death models where the excited state decays with unit probability as soon as it attains certain critical conformations, and (B) finite decay models, where the decay from the critical geometries occur at a finite rate ($=k_0$). All the models belonging to class (A) predict inverse friction (ζ) dependence of the nonradiative decay rate if the radiative relaxation is neglected. These models predict that the long time decay rate is independent of the excitation wavelength although the average rate (so the quantum yield) show a strong dependence. The relaxation behavior of models (B) is controlled by the dimensionless parameter $\tilde{k}_0 (= k_0\zeta/\omega^2\mu$, where ω is the frequency of the excited state surface and μ is the effective mass of the reactive motion). A fractional friction dependence of the long time rate is obtained at low to intermediate values of $\tilde{k}_0$, but an inverse friction dependence is predicted for large values of this parameter. The fractional dependence of the *average* rate on viscosity is found to depend critically on the wavelength of the exciting light. A small negative activation energy is found at small values of $\tilde{k}_0$. A delta-function sink (DFS) is introduced to simplify numerical calculations. This DFS model retains the essential features of the more realistic Gaussian sink model. The DFS model is studied both analytically and numerically. We find that the asymmetry in the position of the sink function, with respect to the minimum of the excited state potential surface, can play an important (hidden) role in the relaxation process. Especially, it can give rise to a significant temperature coefficient of the rate and can lead to an erroneous conclusion on the "molecular" activation energy. Finally, systematics of fitting the experimental data to the present theories are discussed.

I. INTRODUCTION

An electronic relaxation in solution in the absence of an activation barrier is one of the simplest chemical reactions in the liquid phase. In recent years, several such reactions have been studied by using various spectroscopic techniques.[1–15] These studies have revealed diverse and interesting properties. They include the dependence of the relaxation on the solvent viscosity,[1–9] the solvent polarity,[9–12] on the temperature,[8,11–14] and also on the wavelength of the exciting light.[10–12] In this paper a theoretical study of the basic aspects of the relaxation behavior of the barrierless processes in the solution is presented.

Since the motion along the reaction coordinate proceeds here without the intervention of a high barrier, the relaxation may depend critically on the initial conditions. Thus, not only the excitation wavelength but the relative positions and the frequencies of motion of the participating potential surfaces are also important in the dynamics subsequent to excitation. The situation is further complicated here by our lack of precise knowledge of the nature and the positions of the decay channels on the excited state potential surface. It is believed[15,16] that the decay from the excited state surface takes place most efficiently from certain critical geometries (or conformations) of the excited molecule. These geometries serve as "funnels" or "holes" of the excited state potential surface. Moreover, in the absence of a high barrier to the reactive motion, there is no natural separation of time scales between the motion in the reactive region and in the rest of the potential surface.

In these circumstances the scope of any quantitative (theoretical) calculation that can be compared directly with experiments is somewhat limited. Moreover, in the absence of reliable information about the potential surfaces involved, the predictions are bound to be model dependent. Thus, we must seek a minimal set of parameters that can describe the essential characteristics of the potential surfaces. In the theoretical calculations of the sort described here, these parameters will be associated with the reactive molecule, although they must also change as the nature of the solvent is changed. It appears that this minimal set must consist of the following. First, a distance parameter to give the average initial position of the system on the excited surface. Secondly, a frequency to characterize the force experienced by the system on the excited surface. We need two other parameters to characterize the sink function: the rate of decay from the sink and the position of the sink. The last one does not arise if the sink function is placed at the minimum of a symmetric excited state surface. Moreover, the number of "molecular" parameters can be reduced for some simple models appropriate for specific systems, as discussed later.

The existing models of barrierless reaction can be divided into two classes: (A) The instantaneous death models where the excited state decays with unit probability as soon as it reaches certain critical geometries. (B) The finite decay models where the rate of relaxation from the sink region is finite and comparable with the rate of energy relaxation of

[a)] Contribution number 447 from the Solid State and Structural Chemistry Unit.

 0021-9606/87/215393-10$02.10

the system in the excited state potential surface. Next we elaborate on these two different classes.

There exist three models that belong to the class of instantaneous death models [class (A)]. They are: the pinhole sink model introduced by Bagchi *et al.*,[17] the staircase model introduced recently by the author[18] and thirdly, the Oster–Nishijima model[2] introduced about three decades ago. There also exist three models that belong to the class of finite decay models [class (B)]. They are: the quadratic sink model introduced by Förster and Hoffmann,[1] the Gaussian sink model and the Lorentzian sink model, the last two were introduced by Bagchi *et al.*[17] Of these models, the Gaussian sink is obviously more realistic.[19] In this paper we shall use a limiting form of the Gaussian sink model, the delta function sink, which is obtained by taking the width of the Gaussian sink infinitesimally small. The delta function sink model is much simpler to solve numerically and it retains the essential features of the finited decay models. Detailed numerical and analytical study of this model will be presented for the first time.

Note that all the models of class (A) category are essentially two parameter models. Pinhole sink requires that only the initial position of the system and the frequency of the potential surface be specified. Both the staircase and the Oster–Nishijima models depend on the length separating the barriers and on the initial position. On the other hand, the models belonging to class (B) require all the four parameters discussed earlier, except for the limiting case when the sink function is placed symmetrically at the minimum of the harmonic surface. Analytic solution is possible for models (A), but models (B) have to be solved numerically.

The delta-function sink model introduced here has several simplifying features. The main advantage is that one can treat a *displaced sink* on a harmonic potential surface without involving major computational difficulties. The displaced sink may mimic the situation where a *small* activation barrier to the reactive motion is present, as described in Fig. 1. We find that the asymmetry in the position of the sink plays a kind of "hidden" role in the dynamics of relaxation. We shall discuss this point in detail later.

Our theoretical description is based on the following modified Smoluchowski equation description for the probability distribution function $P(x,t)$;

$$\frac{\partial P(x,t)}{\partial t} = \mathscr{L}P(x,t) - k_0 S(x)P(x,t) - k_r P(x,t) \quad (1)$$

with the following notation. x is the one dimensional reaction coordinate, $S(x)$ is the position dependent sink function, k_0 the nonradiative rate of decay from the sink, and k_r is the radiative decay rate from the excited state potential surface. For a harmonic potential of frequency ω, the Smoluchowski operator takes the following form:

$$\mathscr{L} = A\frac{\partial^2}{\partial x^2} + B\frac{\partial}{\partial x}x, \quad (2)$$

where $A = k_B T/\zeta, B = \omega^2\mu/\zeta, \zeta$ is the relevant friction parameter, μ is the effective mass, k_B is Boltzmann constant, and T is the temperature. For both the Oster–Nishijima and the staircase models, B is equal to zero and the dynamics is governed by a diffusion equation with proper boundary conditions. Note that the instantaneous death models [class (A)] can be obtained from Eq. (1) by taking the limits that the width of the sink function goes to zero and the rate k_0 goes to infinity simultaneously.

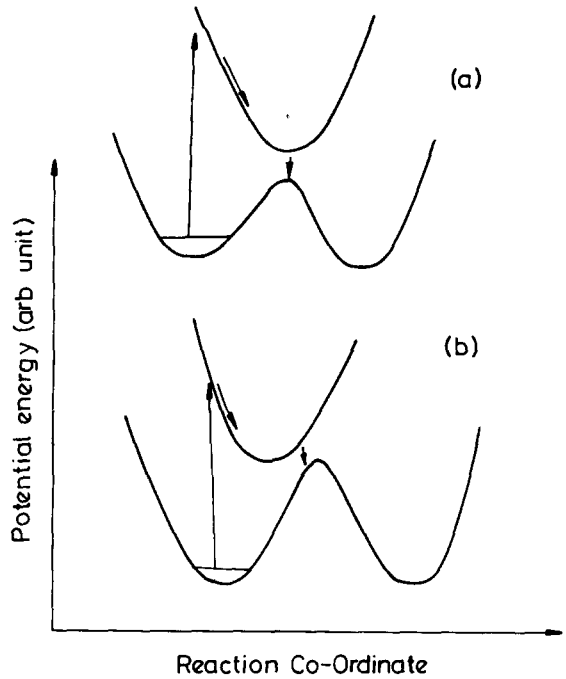

FIG. 1. Schematic illustration of the potential surfaces in which the nonradiative relaxation occurs from (a) symmetric sink ($x_s = 0$), (b) displaced (asymmetric) sink ($x_s \neq 0$).

An interesting aspect of the relaxation in the absence of a high activation barrier is that there is no clear separation of time scales between the motion in the reactive region (which in this case is the sink region) and in the rest of the potential surface. Thus, the relaxation may depend strongly on the initial conditions which means that there may be strong dependence on the wavelength of the exciting light. In this case, therefore, the traditional definition of rate constant in terms of a steady flux across the reactive region may not be applicable. A steady state can still be reached in the long time which, however, may be difficult to detect because the signal may become too low in that limit. It is, therefore, useful to introduce two different rate constants. The first one is the average rate constant, k_I, defined through

$$k_I^{-1} = \int_0^\infty dt\, P_e(t), \quad (3)$$

where $P_e(t)$ is the population remaining on the excited state surface at a time t after the excitation. The second is the long time rate constant k_L, defined through the long time limit of $P_e(t)$,

$$k_L = -\lim_{t\to\infty} \frac{\partial}{\partial t} \ln P_e(t). \quad (4)$$

There may be situations where these two rate constants will be significantly different from each other. It is important to realize that both these two rate constants will contain somewhat different informations. Note that in the present situation, the fluorescence quantum yield is not uniquely defined. Approximately, ϕ_f is related to k_I by the following relation:

$$\phi_f \simeq k_r/k_I, \tag{5}$$

where k_r is the radiative rate. For chemical reactions in the absence of a barrier, the fluorescence quantum yield may depend strongly on the initial conditions. However, ultrafast measurements will be necessary to extract k_I from ϕ_f. Our calculations show that k_I, hence ϕ_f, is affected most by the nonsteady state dynamics which is the hallmark of barrierless reactions. Another rate constant that is used sometimes[22] is the inverse of the average survival time defined by

$$k_a^{-1} = \int_0^\infty dt\, tP_e(t) \Big/ \int_0^\infty dt\, P_e(t). \tag{6}$$

Note that for an exponential decay, all three rate constants are identical.

Although the theoretical results presented here are especially relevant for the photochemical barrierless reactions, they may also find use in other kinds of reactions.[20,21] Recently Sumi and Marcus[22] used an approach similar to the ones employed here to investigate solvent relaxation effects on electron transfer reactions in liquid. Agmon and Hopfield[23] applied essentially the same formalism to study CO rebinding to heme in myoglobin.

The organization of the rest of the paper is as follows. In Sec. II we present the analytical results for all three instantaneous death models. In Sec. III we present theoretical results for the finite decay models. In Sec. IV we present numerical results for instantaneous death models, and in Sec. V for the finite decay models. Section VI concludes with a discussion on the systematics of fitting experimental results to the present theories.

II. THEORY: INSTANTANEOUS DEATH MODELS

In this section we shall present the necessary expressions of the excited state population density $P(x,t)$ for an arbitrary initial population density $P_0(x)$. All the three models belonging to this class are considered.

A. Pinhole sink

In this case we need to solve Eq. (1) [with $\mathscr{L}$ given by Eq. (2)] for the following initial-boundary values:

$$P(x,t=0) = P_0(x), \tag{7a}$$

$$P(x = \pm\infty, t) = 0, \tag{7b}$$

$$P(x=0,t) = 0. \tag{7c}$$

It is straightforward to solve this problem by method of images.[24] The total population remaining on the excited state after time t, $P_e(t)$, is given by

$$P_e(t) = \exp(-k_r t) \times \int_0^\infty dx' [P_0(x') + P_0(-x')]\,\mathrm{erf}\,F(x',t), \tag{8}$$

where

$$F(x,t) = \left[\frac{B}{2A(1-e^{2Bt})}\right]^{1/2} x\, e^{-Bt}. \tag{9a}$$

The error function erf a, is defined by

$$\mathrm{erf}\, a = \frac{2}{\sqrt{\pi}} \int_0^a dy\, e^{-y^2}. \tag{9b}$$

The expression of the two rate constants, k_I and k_L, and other predictions of this model will be discussed in Sec. IV. Here we note that a simple expression can be obtained for $P_e(t)$ when $P_0(x)$ is given by the equilibrium probability distribution on the excited state surface. In that case $P_e(t)$ is given by

$$P_e(t) = \frac{2}{\pi} \tan^{-1}(e^{-Bt}). \tag{10}$$

This expression was first obtained by Schulten, Schulten, and Szebo.[25]

B. Staircase model

In this case, reactive motion occurs on a flat surface ($B=0$). We choose the coordinate system such that the reflecting barrier is at the origin and the absorbing barrier is at $x=a$. The initial boundary

$$P(x,t=0) = P_0(x), \tag{11a}$$

$$\frac{\partial P}{\partial x}(x,t)|_{x=0} = 0, \tag{11b}$$

$$P(x=a,t) = 0. \tag{11c}$$

This problem can be solved by the method of repeated reflections and is given by

$$P(x,t) = \int_0^a dx'\, P_0(x') P(x,t\,|x'), \tag{12a}$$

$$P(x,t\,|x') = \exp(-k_\gamma t)(4\pi A t)^{-1/2} \times \sum_{k=-\infty}^{\infty} (-1)^k \left\{\exp\left[-\frac{(x-x'+2ka)^2}{4At}\right] + \exp\left[-\frac{(x+x'+2ka)^2}{4At}\right]\right\}. \tag{12b}$$

The total population on the excited state surface after time t, $P_e(t)$, is obtained by integrating $P(x,t)$ which leads error functions.[18] However, it is convenient to simplify Eq. (12b) by using Poisson summation.[26] The resulting expression for $P_e(t)$ is now given by

$$P_e(t) = \frac{4}{\pi} \exp(-k_r t) \sum_{n=0}^{\infty} (-1)^n \sum_{n=0}^{\infty} \frac{1}{2n+1} \times \exp\left[-\frac{(2n+1)^2\pi^2}{4a^2} At\right] \times \int_{-\infty}^{\infty} dx' \cos\frac{(2n+1)\pi x'}{2a} P_0(x'). \tag{13}$$

The integral in Eq. (13) can be evaluated in some limiting cases which will be discussed in Sec. IV along with the predictions of this model and expressions of the rate constants.

C. Oster–Nishijima model

In this case the reactive motion is on a flat surface ($B=0$). The initial-boundary values are given by

$$P(x,t=0) = P_0(x), \tag{14a}$$

$$P(x=0,t) = 0, \tag{14b}$$

$$P(x=a,t) = 0. \tag{14c}$$

The coordinate system is such that one absorbing barrier is

at $x=0$ and the other at $x=a$. As before, the solution can be obtained by method of repeated reflections and $P(x,t)$ is still given by Eq. (12a) with a different $P(x,t\,|x')$ which is now given by

$$P(x,t\,|x') = \exp(-k_r t)\,[4\pi A t\,]^{-1/2} \times \sum_{k=-\infty}^{\infty} \left\{ \exp\left[\frac{(x-x'+2ka)^2}{4At} \right] - \exp\left[-\frac{(x-x'+2ka)^2}{4At} \right] \right\}. \tag{15}$$

This can also be transformed to a more convenient form by using Poisson summation formula. The final expression for the survival probability $P_e(t)$ is given by

$$P_e(t) = \frac{4}{\pi} \exp(-k_r t) \sum_{n=0}^{\infty} \frac{1}{2n+1} \times \exp\left[-\frac{(2n+1)^2 \pi^2}{a^2} At \right] \times \int_{-\infty}^{\infty} dx'\, P_0(x') \sin \frac{(2n+1)\pi x'}{a}. \tag{16}$$

Equation (16) can be simplified in some limiting case. This will be discussed, along with the expressions of the rate constants and the other predictions of this model in Sec. IV.

III. THEORY: FINITE DECAY MODELS

In this section we shall consider both the Gaussian sink and the delta function sink models with more emphasis on the latter. Some aspects of the earlier treatment of the Gaussian sink model[17,19] will be clarified and the results will be made more compact.

The general Gaussian sink can be represented by a Gaussian function centered at a position x_s,

$$S(x) = \frac{1}{\sigma\sqrt{\pi}} \exp[-(x-x_s)^2/\sigma^2]. \tag{17}$$

It was discussed at length in Ref. 19 why this functional form is realistic. Note that we have made minor changes from the form given in Ref. 19. The delta-function sink is obtained by taking the limit $\delta \to 0$,

$$S(x) = \delta(x - x_s) \tag{18}$$

with the sink functions (17) and (18), it has not been possible to solve Eq. (1) analytically. However, a convenient numerical method to solve Eq. (1) is to expand $P(x,t)$ in the eigenfunctions of the operator. The details are given in Refs. 17 and 19.

We shall now discuss some general aspects of the finite decay models. Note that Eq. (1) contains *three* time constants A^{-1}, B^{-1}, and k_0^{-1} (with ζ as the rotational friction). The last two, B^{-1}, and k_0^{-1}, depend strongly on the molecular potential surface, B^{-1} through ω^2 and k_0^{-1} through the energy gap between the two participating surfaces. At low friction, three time constants may be of the same order of magnitude for many systems, especially for TPM dyes[11] and for *trans*-stilbene. At very low values of ζ (which may be realizable for *trans*-stilbene in lower *n*-alcohols), the rate may be limited by k_0. In this limit, the rate of relaxation will *decrease* with *increase* of temperature, that is, we will have an apparent negative activation energy. The explanation for this is very simple—the increase in temperature broadens the distribution in the sink region, thus removing population from the position where the decay is maximum.

In the large viscosity limit, the rate will be controlled by A and B, especially by B in the long time limit. It is convenient to transform Eq. (1) to the following form:

$$\frac{\partial P}{\partial t_1} = \tilde{A} \frac{\partial^2 P}{\partial x^2} + \frac{\partial}{\partial x} xP - \tilde{k}_0 S(x) P - \tilde{k}_r P, \tag{19}$$

where

$$t_1 = Bt, \quad \tilde{A} = A/B, \quad \tilde{k}_0 = k/B, \quad \tilde{k}_r = k_r/B. \tag{20}$$

Equation (19) is now in dimensionless form (for rotational diffusion). Equation (19) is suitable for studying the general relaxation properties. Note that $\tilde{A}$ is independent of friction. If a long time rate constant k_L exists, then scaling analysis gives (for $k_r = 0$)

$$k_L \simeq B f(\tilde{A}, \tilde{k}_0), \tag{21}$$

where the function f depends on friction through its dependence on the dimensionless quantity $\tilde{k}_0 (= k_0/B = k_0\zeta/\omega^2\mu)$. In the following analysis, we shall assume that $\tilde{A} (= k_B T/\omega^2\mu)$ is constant, that is, we vary friction at constant temperature. In the limit $\tilde{k}_0 \gg 1$, f approaches unity and $k_L \simeq B$, i.e., inverse dependence on friction. In the other limit, $k_0 \ll 1$, $f \sim k_0/B$, and $k_L \sim k_0$, that is, the rate become independent of friction. In Sec. V we shall confirm this limit by explicit numerical calculation. The behavior of the integrated rate constant $\tilde{k}_I$ remains close to $\tilde{k}_L$ in the small friction regime, but deviates significantly from $\tilde{k}_L$ when friction becomes large ($\tilde{k}_0 \gg 1$). $\tilde{k}_I$ shows fractional friction dependence for a wider range of $\tilde{k}_0$ than observed for $\tilde{k}_L$. The differences between k_I and k_L are hallmarks of the barrierless reactions and is because of nonsteady state dynamics on the excited state surface.

The main point of the preceding discussion is that the friction dependence of the rate of relaxation is controlled by the ratio k_0/B. A fractional friction dependence of k_L is predicted in the range $1 \leqslant \tilde{k}_0 \leqslant 10$ and in a wider range for k_I. Note that the preceding analysis applies strictly to the dependence of rate on the friction coefficient ζ, and *not* to the observed viscosity dependence of the rate. Usually a linear, Stokes–Einstein, relation is assumed between the friction ζ and the viscosity η. However, several recent studies[27–29] have questioned the relationship. The fractional friction dependence predicted in the present theory arises from a competition between the rate of temporal evolution of the population distribution towards its equilibrium form and the rate of removal of the population from the sink region which prevents the distribution from attaining its equilibrium form. Thus, the fractional friction dependence arises as a general feature of our model of barrierless reactions and not from any particular relationship between ζ and η and so in no way is related to the breakdown of Stokes–Einstein relation discussed recently.[28]

We would also like to stress that Eq. (23) predicts nonexponential behavior at short times. In the limit of long time (that is, $Bt > 1$), a single exponential behavior is recovered

because a steady state will be reached. This has been confirmed numerically.

Next, we consider the different sink functions separately.

A. Delta-function sink at origin

In this case the matrix elements I_{mn} are simple and given by (in the notation of Ref. 17)

$$I_{mn} = H_n(0)H_m(0), \tag{22}$$

with the following expression for $H_n(0)$,

$$H_{2n}(0) = (-1)^n \frac{2n!}{n!}, \tag{22a}$$

$$H_{2n+1}(0) = 0. \tag{22b}$$

Let us define matrix elements J_{nm},

$$J_{mn} = A_m^{1/2} A_n^{1/2} I_{mn}. \tag{23}$$

In the present case J_{nm} remains bounded and small for large values of n and m, making numerical calculations simple. Numerical results will be presented in Sec. V.

B. Asymmetric delta-function sink

In This case the sink is at $x = x_s$. The matrix elements are given by

$$I_{mn} = \exp(-x_s^2/2V^2) H_m\left(\frac{x_s}{V\sqrt{2}}\right) H_n\left(\frac{x_s}{V\sqrt{2}}\right). \tag{24}$$

For large m and n, the following asymptotic expansion of Hermite polynomials[30] will prove useful:

$$H_n(y)H_n(y) \overset{y\to\infty}{\sim} 2^{(n+1)/2} e^{y^2/2} \left(\frac{n}{e}\right)^{n/2} \times \cos\left[y\sqrt{2n+1} - \frac{n\pi}{2}\right]. \tag{25}$$

Thus, the matrix elements J_{nm} [defined by Eq. (23)] also remain bounded and small for large n and m. Since $x_s^2/V^2 = \mu\omega^2 x_s^2/k_B T$, the exponential in Eq. (24) has the form of activation energy. However, asymptotic expansion of Hermite polynomials show that this term gets canceled for large n and m. We shall show by explicit numerical calculations in Sec. V that the asymmetry in the position of the sink can have stronger effects than what can be anticipated by usual arguments.

C. Gaussian sink at the origin

The relaxation behavior of this model was considered in Ref. 17 in detail. Here we analyze some aspects of this model not considered earlier. In order to make connection with earlier work, we set

$$k_{nr} = k_0/a\sqrt{\pi}, \tag{26}$$

$$J'_{mn} = k_{nr} A_m^{1/2} A_n^{1/2} I_{mn}. \tag{27}$$

Note that the delta-function sink is recovered if we take the limit $\sigma \to 0$, $k_{nr} \to \infty$ simultaneously, and pinhole sink is recovered from delta function sink by taking $k_0 \to \infty$.

Here we shall consider small σ. In this limit, the first three coefficients, J_{mn}s of Eq. (27), are given by

$$J'_{00} = \left(\frac{B}{2\pi A}\right)^{1/2} k_{nr}, \tag{28a}$$

$$J'_{02} = J'_{20} = -\frac{1}{2}\left(\frac{B}{\pi A}\right)^{1/2} k_{nr}, \tag{28b}$$

$$J'_{22} = \frac{3}{2}\left(\frac{B}{2\pi A}\right)^{1/2} k_{nr}. \tag{28c}$$

A simple analysis shows that a single exponential behavior can occur at large B if $B \gg k_{nr}(J'_{00} + J'_{22})$. This condition may not be satisfied for most experimental conditions (and definitely not for TPM dyes in alcohols). This has created some confusion.[11,31] It is important to realize that any narrow sink will always give rise to single exponential decay for $Bt \gg 1$. For large B (small ζ), the separation between the lowest eigenvalue of the relaxation matrix and the next higher eigenvalue is large compared to that for small B.[17] Thus, we predict increasing nonexponential behavior as B is decreases. The next important point is that if k_r is neglected, then theory predicts inverse viscosity dependence of k_L for large k_0. The situation is somewhat different for k_I which depends strongly on the excitation wavelengths. This shall be discussed in the next section.

IV. RESULTS: INSTANTANEOUS DEATH MODELS

Analytical expressions for $P_e(t)$ is given in Sec. II for all the models belonging to this class. In the following we discuss quantitative aspects of the dependence of relaxation on excitation wavelength, temperature, and viscosity.

A. Temporal profile and rate constant

All the three models, the pinhole sink, the Oster–Nishijima, and the staircase models, predict multiexponential behavior at short times ($Bt \simeq 1$ for pinhole sink, and $At/a^2 \simeq 1$ for ON and S models), but single exponential behavior at long times. However, the approach to equilibrium is different in the three models. In the case of pinhole sink, the long time decay is dominated by Bt, where in the other two cases, the long time decay is governed by $\nu(\pi^2 A/a^2)t$, ν being 1 for the ON model and 1/4 for the staircase model.

In order to evaluate $P_e(t)$ and the rate explicitly, we need an expression for $P_0(x)$. If we assume that the ground state potential well is harmonic, then a reasonable approximation is

$$P_0(x) = \frac{1}{\gamma\sqrt{2\pi}} \exp[-(x - x_0)^2/2\gamma^2], \tag{29}$$

with

$$\gamma^2 = k_B T/\omega_g^2, \tag{30}$$

ω_g being the frequency of the ground state surface and x_0 is the position of the minimum of the ground state surface.

With the above form of $P_0(x)$, the relevant expressions can be computed. For pinhole sink, we have (for $k_r = 0$)

$$P_e(Bt \gg 1) \sim \frac{2}{\sqrt{\pi}} \langle x_0 \rangle \left(\frac{B}{2A}\right)^{1/2} e^{-Bt}. \tag{31}$$

So

$$k_L = B. \tag{32}$$

The integrated rate is given by

$$k_I^{-1} = \frac{1}{B\sqrt{\pi}} \sum_{n=0}^{\infty} (-1)^n \frac{M_{2n+1}(B/2A)^{n+1/2}}{n!(2n+1)!} \times \frac{\Gamma(n+\frac{1}{2})}{\Gamma(2n+2)}, \quad (33)$$

where

$$M_{2n+1} = \frac{1}{\gamma\sqrt{2\pi}} \int_0^{\infty} dx\, x^{2n+1} \times [e^{-(x-x_0)^2/2\gamma^2} + e^{(x+x_0)^2/2\gamma^2}]. \quad (33a)$$

Expressions for k_L and k_I can be obtained for the other two models.

In Fig. 2 we have plotted $P_e(t)$ of the pinhole sink model for a delta-function source at $x = x_0$ and for a finite width source of form (29). Note that an initial distribution of finite width (nonzero γ) can lead to considerably faster decay at short times. This will be true irrespective of the model studied.

In Fig. 3 we have plotted $P_e(t)$ for the ON and the S model for a delta-function source at x_0. The difference between the two models is most dramatic if x_0 is close to the origin. In that case the integrated rate constant k_I for the ON model can be much larger than that for the S model.

We would like to stress that all the models belonging to the class of instantaneous death models predict an inverse dependence of both k_I and k_L. Thus, detailed experimental study of $P_e(t)$ and its dependence on the excitation wavelength would be necessary to find out which of these models is appropriate for a given experimental situation.

B. Excitation wavelength dependence

The dependence of reaction dynamics on the wavelength of the exciting light enters through the initial population distribution $P_0(x)$. A word of caution is warranted here. The relationship between $P_0(x)$ and the wavelength of the exciting light may not be as straightforward as depicted here because most reaction surfaces would be multidimensional. However, there now exist some experimental results that indicate a significant dependence of decay on the wavelength

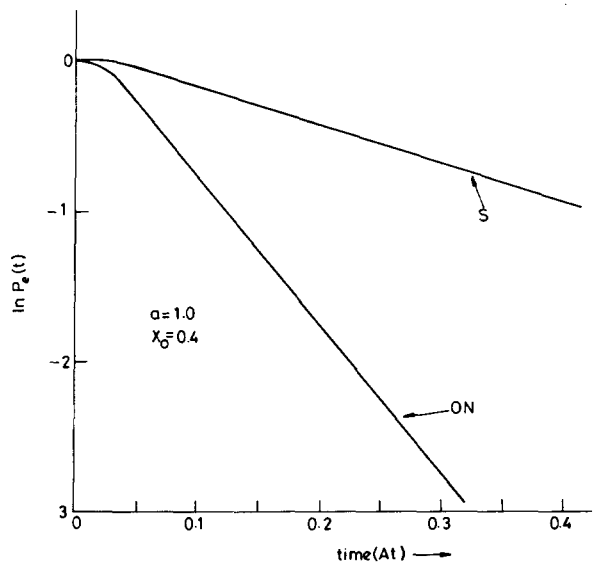

FIG. 3. The decay profile of Oster–Nishijima (ON) model is compared with that of the staircase (S) model. The parameter values are given in the figure.

of the exciting light.[11,32] In the following we briefly discuss the kind of dependence predicted by the models in question.

First, note that all the models in question predict that the long time decay rate k_L is independent of $P_0(x)$. The integrated rate constant k_I, on the other hand, depends strongly on $P_0(x)$ for all the models being discussed here. In Fig. 4 we have plotted k_I, of both ON and S models, against x_0 (with a delta function source at x_0). The dependence on x_0 is quite different in the two cases. This difference may prove to be useful in the experimental study of the excitation wavelength dependence. Especially, they may be useful in the extraction of important molecular parameters. A significant wavelength dependence may provide us with an important inroad into the nature of the decay channels operating in a particular relaxation process.

C. Temperature dependence

The temperature dependence of relaxation enters in two ways in the present description. First, the diffusion param-

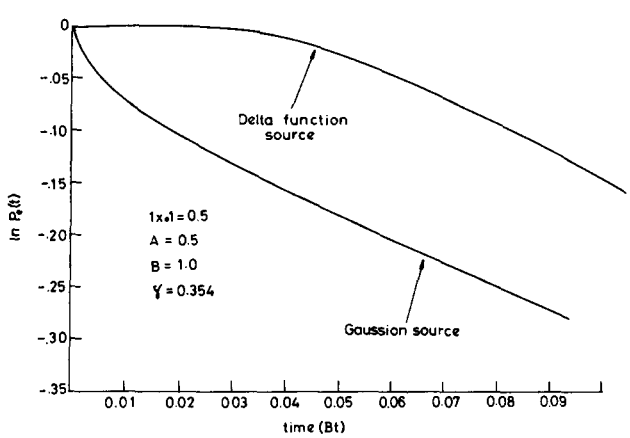

FIG. 2. The short time decay of the excited state population is plotted for a Gaussian source (nonzero γ) and for a delta function source, for a pinhole sink. The parameter values are given in the figure.

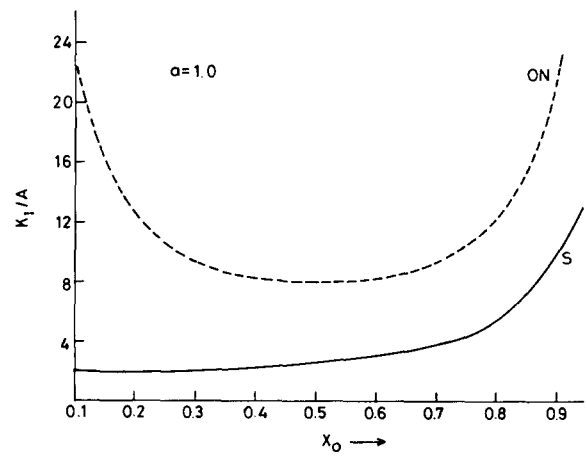

FIG. 4. The values of the integrated rate constant k_I are plotted against the source position x_0 for both the Oster–Nishijima (ON) and the staircase (S) models. The rate is expressed in the unit of $A(=k_BT/\zeta)$.

eter $A(=k_BT/\zeta)$ changes linearly with temperature. Secondly, the initial distribution $P_0(x)$ broadens as temperature is increased. In the following discussion we shall assume that the frequency of the excited surface and the position of the sink(s) do not change with temperature. Thus, we shall examine the effects arising solely from the change of temperature.

For the pinhole sink, the long time decay constant (k_L) is independent of temperature at constant viscosity. The broadening of $P_0(x)$ and increase of A would lead to a faster initial decay, so k_I would increase with temperature. For Oster–Nishijima model, both k_L and k_I have positive temperature coefficient, if ζ is kept constant. This is true at all viscosities. For the staircase model, k_L increases with temperature, but k_I would be less sensitive than the ON model for small x_0 (average source position for a Gaussian source), as evident from Fig. 4.

V. RESULTS: FINITE DECAY MODELS

In this section we present numerical results for both the symmetric delta-function sink model (sink at the origin) and the displaced delta-function sink model. The latter corresponds to an activated process, but we are interested only at small barriers so that the nonsteady state dynamics is important and Kramers' regime is not achieved. In both the two cases, we solved the linear system of equations numerically. For the symmetric sink, only the even eigenstates are coupled. At large values of $\tilde{k}_0 (2 \simeq \tilde{k}_0 < 50)$, we need a large number (60–100) of the even eigenstates to obtain convergence. For the displaced sink, however, all the eigenstates are coupled and we found it difficult to obtain convergence at large values of $\tilde{k}_0$. Because of the limitation on our computer memory, we were restricted to intermediate values of $\tilde{k}_0$ for the displaced sink. The eigenvalues of the rate matrix are obtained by straightforward diagonalization. We found it more convenient to obtain k_I by direct matrix inversion. All the computation was done on a DEC-1090 computer at I.I.SC. Bangalore.

A. Delta-function sink at origin

1. Nonsteady state dynamics and multiexponential decay

The condition of a single exponential decay is that the lowest eigenvalue λ_1 should be substantially smaller than the next higher, eigenvalue λ_2. Thus, a suitable parameter to study multiexponential decay is given by

$$\Delta_{12} = (\lambda_2 - \lambda_1)/\lambda_1. \tag{34}$$

For single exponential decay to dominate the overall relaxation process, Δ_{12} must be much greater than unity. This is also the condition for a steady (constant) rate of decay from the sink region.

In Fig. 5 we have plotted the values of Δ_{12} against $\tilde{k}_0 (= k_0/B)$. The insert in this figure is for very small values of $\tilde{k}_0$. It is seen clearly that Δ_{12} becomes very large at small values of $\tilde{k}_0$ indicating a single exponential behavior. At larger values of $\tilde{k}_0 (k_0 \geqslant 2)$, Δ_{12} gets smaller and becomes comparable to unity. It is in this range that the multiexponential

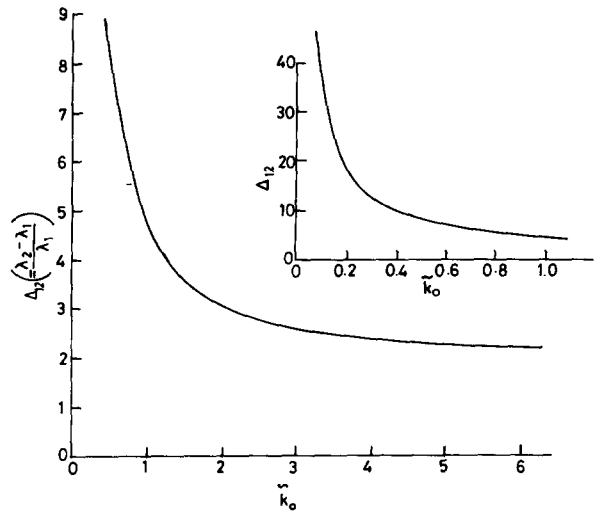

FIG. 5. The calculated values of Δ_{12}, defined by Eq. (34), are plotted against k_0 for the symmetric delta-function sink. The inset in the figure shows the behavior for small values of $\tilde{k}_0$ on an expanded scale. $\tilde{A} = 0.5$.

behavior begins to dominate the relaxation process. In Fig. 6 we have plotted the time dependent excited state population $P_e(t)$ against time for three values of $\tilde{k}_0$. The increasing nonexponential character of the decay, as $\tilde{k}_0$ is increased, is clear from the graphs.

Since the results are given in terms of the dimensionless quantity $\tilde{k}_0$, there are two ways to interpret the results. First, we can keep B (i.e., the friction) constant and vary k_0. Alternatively, we can fix k_0, and change B. In the latter case, Figs. 5 and 6 depict the effects of changing viscosity on the relaxation process. As friction increases, B decreases and $\tilde{k}_0$ increases. So, low $\tilde{k}_0$ corresponds to low friction and large $\tilde{k}_0$ corresponds to large friction. Thus, Fig. 6 shows the crossover to nonexponential behavior as ζ increases. This has been observed experimentally in some cases and discussed theoretically in our earlier papers. Note that the scale changes in Fig. 6 as B is changed. For larger $\tilde{k}_0$, B is also larger. At large values of $Bt (Bt > 1)$, the relaxation becomes single exponential or all $\tilde{k}_0$. However, the signal in this re-

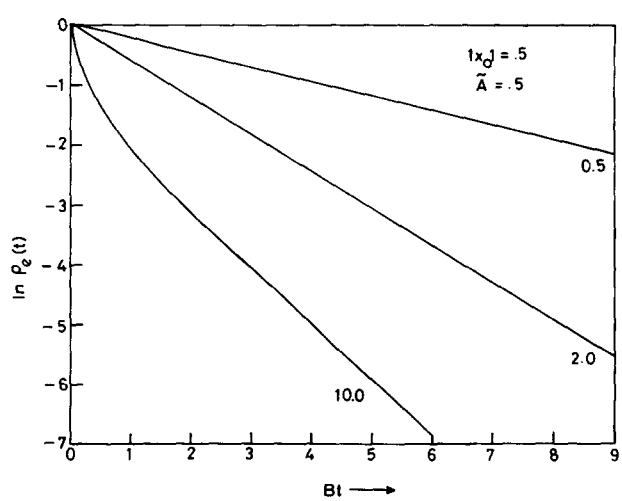

FIG. 6. The excited state population $p_e(t)$ is plotted against Bt for several values of the dimensionless quantity $\tilde{k}_0$ for the symmetric delta-function sink. $\tilde{k}_0$ values are given in the figure $x_0 = 0.5$.

gion may become too low in some cases to detect this long time single exponential behavior.

2. Nonsteady state dynamics and fractional viscosity dependence of rate

We present two important results here. The first one is concerned with the significantly different viscosity dependence of the two rate constants k_L and k_I. Secondly, we find that, for k_I, the viscosity dependence is a function of the excitation wavelength. That is, k_I is a function of both x_0 and ζ.

In Fig. 7, we have plotted both the lowest eigenvalue $\tilde{\lambda}_1 = (= \tilde{k}_L)$ and the integrated rate constant $\tilde{k}_I$ against $\tilde{k}_0$. The values of $\tilde{k}_I$ are given for several values of the initial position x_0. As $\tilde{k}_0$ becomes larger, $\tilde{\lambda}_1$ approaches unity which means λ_1, and k_L, become equal to B. This is, of course, expected from the known result for the pinhole sink. Thus, k_L has a viscosity dependence of the form $k_L \propto \eta^{-\alpha}$ (with exponent α less than unity) only for high values of B. Thus, at fixed k_0, a fractional viscosity dependence of k_L is predicted only at *small* viscosities, in agreement with the theoretical analysis presented earlier in this section.

However, the behavior of k_I is significantly different from that of k_L. First, the values of k_I seem to saturate at *larger* values of $\tilde{k}_0$ which means fractional viscosity dependence will be observed over a *larger* range of viscosity. Secondly, the variation of $\tilde{k}_I$ with $\tilde{k}_0$ depends strongly on the initial condition. For example, for $x_0 = 0.1$, the fractional viscosity dependence is predicted even beyond $\tilde{k}_0 \geqslant 50$. This seems to be in the range available to experimental studies. For TPM dyes, $\simeq 10^{10}$–10^{11} s^{-1} at $\eta = 1$ cp if the reactive motion is a synchronous rotation of the phenyl rings, and $k_0 \simeq 10^{12}$ s^{-1}. However, $\tilde{k}_0$ may also change with viscosity because a change in viscosity is usually accompanied by a change of the dielectric properties of the solvent. Thus, although we predict a fractional dependence of k_I, it is not possible, within this theory, to attribute it solely to viscous effects.

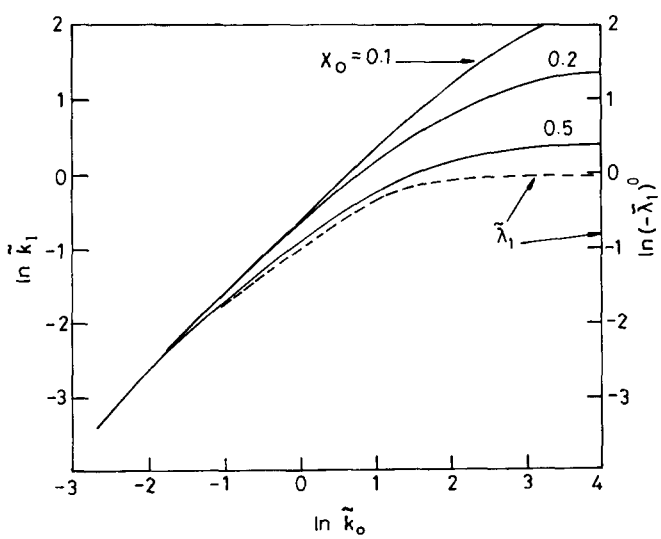

FIG. 7. The calculated values of $\tilde{\lambda}_1$ and $\tilde{k}_1$ are plotted against $\tilde{k}_0$ for the symmetric delta-function sink. $\tilde{k}_I$ is plotted for several values of the initial position x_0 on the excited state potential surface. The values of x_0 are indicated on the graph.

The preceding discussion suggests that experimental analysis of the viscosity dependence should be carried out by obtaining both k_I and k_L (if single exponential decay is attained at long times) as functions of viscosity at various excitation wavelengths in similar (in polar properties) solvents. At the viscosity usually attained in experiments and for the type of molecules that undergo barrierless reactions via large amplitude motion, the present model predicts that the *long time decay k_L will probably show inverse viscosity dependence at all viscosities.* But k_I may show fractional viscosity dependence at small to intermediate values of viscosity. Moreover, k_I may show a dependence on the excitation wavelength but k_L should be independent of it.

We would like to stress here that if an instantaneous death model is appropriate for a given situation, then an inverse viscosity dependence would be observed at all viscosities for both k_L and k_I. Thus, careful experimental studies are necessary to understand all these competing factors.

3. Temperature dependence of rate

As low values of $\tilde{k}_0$ an equilibrium (Boltzmann) distribution is attained on the excited state surface before any significant decay can take place. Increase of temperature then widens the Boltzmann distribution and removes population from the sink region, giving rise to a *decrease* in the rate of decay. Thus, we would have an apparent *negative* activation energy at low values of $\tilde{k}_0$. But as $\tilde{k}_0$ is increased, the Boltzmann distribution is never attained, the rate determining step is now the time the system takes to reach the sink and the rate increases with T. Thus, a crossover to positive activation energy is predicted. However, note that k_0 may itself increase with T, thus giving rise to an activation energy larger than what is expected from the above effect along.

B. Asymmetric delta-function sink

The motivation to study this particular model comes from the observation that polar solvents can significantly modify the characteristics of the reactive potential surface.[11,12] In fact, the symmetric sink models considered thus far may not be realistic for most circumstances and reactant–solvent interactions can definitely break the symmetry. Of course, if the effects of asymmetry are not important, then symmetric sink model may suffice. To the contrary, we show in this section that even a small asymmetry has a big effect which is not anticipated from activated kinetics.

In order to study the effect of the position of the sink x_s we have carried out two calculations. In the first calculation we have kept the rate parameter $\tilde{k}_0$ fixed and varied the sink position x_s. In the second calculation we have kept x_s fixed and varied $\tilde{k}_0$.

In Fig. 8, we have plotted the results of our first calculation. Note that the activation energy, measured from the minimum of the excited state surface, is negligibly small for the values of x_s considered in Fig. 8. As can be seen from this figure, displacing the sink has a dramatic effect on the average rage $\tilde{k}_I$. Similar effect is also obtained for the long time

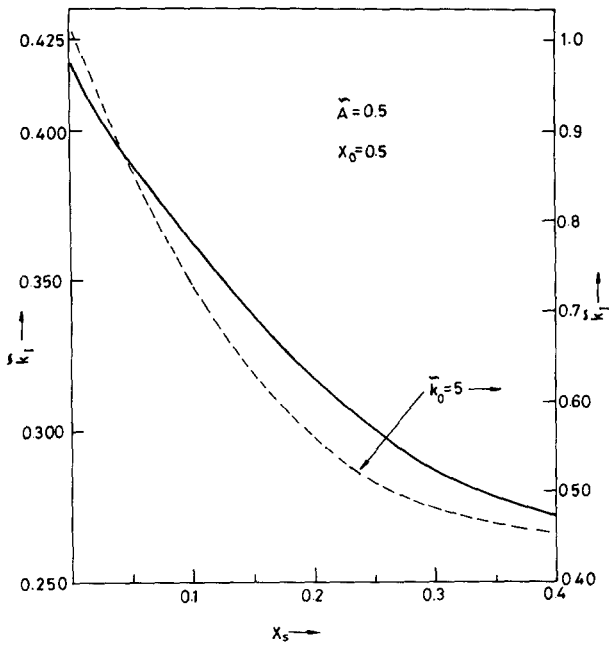

FIG. 8. The values of the integrated rate $\tilde{k}_I$ are plotted against the sink position x_s of the displaced (asymmetric) sink for two values of the rate parameter $\tilde{k}_0$. The dashed line is for $\tilde{k}_0 = 5$ and the solid line for $\tilde{k}_0 = 1$. Note that the ordinate scales are different for the two figures. Values of $\tilde{A}$ and x_0 are given in the figure.

rate constant $\tilde{k}_L$. For both the cases, the effect of asymmetry increases as $\tilde{k}_0$ increases.

In Fig. 9, we have plotted the calculated rate $\tilde{k}_I$ against $\tilde{k}_0$ for several values of x_s. The strong effect of shifting the position of the sink function from $x_s = 0$ is clearly manifested in the graphs.

It should be clear from the above results that the relaxation behavior of an asymmetric sink is quite different from what is expected for an activated rate process. As x_s is increased, the results tend to become similar to an activated process in the sense that the slope of $\ln k_L$ vs x_s^2 gets close to $(2\tilde{A})^{-1}$ at large x_s $(x_s \gg 1)$.

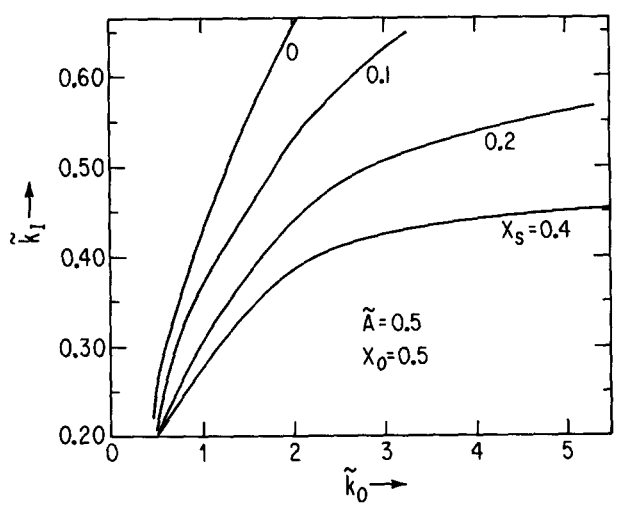

FIG. 9. The values of the calculated rate $\tilde{k}_I$ are plotted against $\tilde{k}_0$ for several values of the sink position, x_s. The values of x_s, x_0, and $\tilde{A}$ are indicated in the figure.

We end this section by emphasizing that if the isoviscous variation of temperature leads to the formation of an asymmetric sink function, then a large temperature coefficient may be observed which may lead to the conclusion of the presence of a large molecular activation energy. This point ceretainly deserves to be studied further.

VI. DISCUSSION

The dynamics of barrierless processes have received much less attention from the theoretical standpoint, compared to the activated processes. Several recent theoretical and experimental studies, however, indicated[22,23,35] that barrierless processes are not limited only to the electronic relaxation in a few aromatic molecules. Thus, the results of the present study may find application to problems in rather different areas, such as in protein dynamics[23,33] and in electron transfer reactions.[22]

One objective of the present study is to understand the predictions of the existing theoretical models for barrierless reactions. Although these models are quite different from each other in their physical content, the quantitative predictions that they offer may be rather similar so that unambiguous experimental judgment in favor of one model or the other is difficult. For example, the Oster–Nishijima and the staircase models both give multiexponential decay with long time rate constants that differ only by a numerical factor. So, if we simply fit the experimental decay function $P_e(t)$ to the theoretical forms for any particular excitation wavelength, equally good fit may be obtained for the two cases. It appears that the only way to decide which of these two models is more appropriate for a given situation is to vary the excitation wavelength (thus vary the initial position x_0). This is, obviously, not a very satisfactory solution.

Fortunately, it may not be very difficult to decide between a finite decay model and an instantaneous death model. A careful study of the temperature dependence of the relaxation process at low viscosity may indicate which type is operating. A negative molecular activation energy would indicate a finite decay model.

All the instantaneous death models are essentially two parameter models. If a good single exponential decay is observed in the long time, then k_L directly gives information about one parameter (ω for pinhole sink, **a** for ON and S models). The other parameter (x_0 for all these models) may be obtained by fitting $p_e(t)$ to theory. A consistency check can be done by comparing x_0 thus obtained to the intercept of $\ln P_e(t)$ vs t plot for large t. For example, for the pinhole sink Eq. (31) gives the intercept as $\ln[2/\pi\langle x_0\rangle (B/2A)^{1/2}]$. Since $B = k_L$, an estimate of x_0 may be obtained. Note that theoretical predictions do not involve friction parameter ζ as an independent entity; ζ always occurs in combinations with other parameters.

The most general model of barrierless reactions is perhaps the displaced sink model discussed earlier. In its simplest form, it involves four parameters: ω, k_0, x_0, x_s. As we have discussed in Sec. V, the sink position can play a "hidden" role in the dynamics of a barrierless process. The displaced sink model may be useful in explaining the large tem-

perature coefficient that has been observed as the nature of the solvent is changed.

In conclusion we note that it is important to gain a quantitative understanding of dynamics of barrierless processes in solution because these processes play important roles in many chemical, physical, and biological systems. Further experimental and theoretical studies on these problems will certainly be worthwhile.

After submitting the paper, the author became aware of three recent publications of Ben-Amotz and Harris on the study of torsional dynamics of triphenyl methane dyes in solution.[34–36] These papers reported extensive study of the dependence of electronic relaxation on solvent viscosity, temperature, and pressure. We hope to compare these experimental results with the theory presented here in a separate publication.

ACKNOWLEDGMENTS

The author thanks Professor Graham Fleming for many interesting discussions and Dr. Villy Sundstrom for useful correspondence. The author is grateful to Professor C. N. R. Rao for encouragement and discussions.

[1]Th. Förster and G. Hoffmann, Z. Phys. **75**, 63 (1971).
[2]G. Oster and Y. Nishijima, J. Am. Chem. Soc. **78**, 1581 (1956).
[3]M. D. Hirsch and H. Mahr, Chem. Phys. Lett. **71**, 27 (1980).
[4]L. A. Brey, G. B. Schuster, and H. G. Drickamer, J. Chem. Phys. **67**, 2648 (1976).
[5]E. P. Ipen, C. V. Shank, and A. Bergman, Chem. Phys. Lett. **38**, 611 (1976).
[6]G. S. Beddard, T. Doust, and M. W. Windsor, in *Picosecond Phenomena II*, edited by R. M. Hochstrasser, W. Kaiser, and C. V. Shank (Springer, New York, 1980), p. 167.
[7]D. A. Cremers and M. W. Windsor, Chem. Phys. Lett. **71**, 27 (1980).
[8]D. A. Cremers, Thesis, Washington State University, 1980 (unpublished).
[9]K. M. Keery and G. R. Fleming, Chem. Phys. Lett. **93**, 322 (1982).
[10]V. Sundstrom, T. Gillbro, and H. Bergstrom, Chem. Phys. **73**, 439 (1982).
[11]V. Sundstrom and T. Gillbro, J. Chem. Phys. **81**, 3463 (1984); Chem. Phys. Lett. **110**, 303 (1984); E. Akesson, H. Bergstrom, V. Sundstrom, and T. Gillbro, *ibid.* **126**, 385 (1986).
[12]J. Hicks, M. Vandersall, Z. Babarogil, and K. B. Eisenthal, Chem. Phys. Lett. **116**, 18 (1984).
[13]D. Ben-Amotz and C. B. Harris, Chem. Phys. Lett. **199**, 305 (1985).
[14]D. Ben-Amotz and C. B. Harris, in *Ultrafast Phenomena*, edited by G. R. Fleming and A. E. Siegman (Springer, New York, 1986).
[15]G. R. Fleming, in *Chemical Applications of Ultrafast Spectroscopy* (Oxford University, New York, 1986), Chap. 6.
[16]N. J. Turro, *Modern Molecular Photochemistry* (Benjamin–Cummings, Menlo Park, California, 1978).
[17](a) B. Bagchi, G. R. Fleming, and D. W. Oxtoby, J. Chem. Phys. **78**, 7375 (1983); (b) B. Bagchi, S. Singer, and D. W. Oxtoby, Chem. Phys. Lett. **99**, 225 (1983); (c) B. Bagchi, *ibid.* **128**, 521 (1986).
[18]B. Bagchi, Chem. Phys. Lett. **135**, 558 (1987).
[19]B. Bagchi, Int. Rev. Phys. Chem. **6**, 1 (1987).
[20]S. G. Entelis and R. P. Tiger, in *Reaction Kinetics in the Liquid Phase* (Wiley, New York, 1976).
[21]B. Bagchi, J. Indian Chem. Soc. **63**, 168 (1986).
[22]H. Sumi and R. Marcus, J. Chem. Phys. **84**, 4894 (1986).
[23]N. Agmon and J. Hopfield, J. Chem. Phys. **78**, 6947 (1983).
[24]M. Leve, *Probability Theory*, 3rd ed. (Van Nostrand, Princeton, 1963).
[25]K. Schulten, Z. Schulten, and A. Szabo, Physica A **100**, 599 (1980).
[26]E. C. Titchmarsh, *The Theory of Functions*, 2nd ed. (Oxford University, Oxford, 1939).
[27]I. Artaki and J. Jonas, J. Chem. Phys. **82**, 3360 (1985).
[28]R. Zwanzig and A. Harrison, J. Chem. Phys. **83**, 5861 (1985).
[29]M. Lee, A. J. Bain, P. J. McCarthy, C. H. Han, J. N. Haseltine, A. B. Smith III, and R. M. Hochstrasser, J. Chem. Phys. **85**, 4341 (1986).
[30]G. Szebo, *Orthogonal Polynominals* (American Mathematical Society, New York, 1939), p. 194.
[31]B. Bagchi, Chem. Phys. Lett. **115**, 209 (1985).
[32]V. Sundstrom (private communication).
[33]D. Beece, L. Eisenstein, H. Frauenfelder, D. Good, M. C. Marden, L. Reinisch, A. H. Reynolds, L. B. Sorensen, and K. T. Yue, Biochemistry **19**, 4147 (1980).
[34]D. Ben-Amotz and C. B. Harris, J. Chem. Phys. **86**, 4856 (1987).
[35]D. Ben-Amotz and C. B. Harris, J. Chem. Phys. **86**, 5433 (1987).
[36]D. Ben-Amotz, R. Jeanloz, and C. B. Harris, J. Chem. Phys. **86**, 6119 (1987).